

Self-consistent calculations of the energy and tunable emission spectra of doping superlattices

Valerii K. Kononenko^{1*}, Dmitrii V. Ushakov², Ivan S. Manak², Philippe Christol³,
and Andre Joullie³

¹ Stepanov Inst. of Physics NASB, Fr. Scorina Ave., 70, 220072 Minsk, Belarus

² Belarussian State Univ., Fr. Scorina Ave., 4, 220050 Minsk, Belarus

³ Univ. de Montpellier II, 34095 Montpellier Cedex 05, France

ABSTRACT

Based on the developed method of self-consistent calculations the results of description of tunable optical spectra versus temperature and excitation level for the GaSb doping superlattices of different design are presented. Account of the appearing tails of the density of states allows describing the long-wavelength edges and shape transformation in the spectra of absorption, gain, and luminescence and peculiarities in the optical transitions characteristics. Possible laser diode structures with *n-i-p-i* crystals in the active region are suggested including ordinary and δ -doped superlattices. Effects of tunable lasing are examined and ways for control of the radiation wavelength are discussed.

Keywords: *n-i-p-i* crystal, potential relief, tail of the density of states, gain spectrum, tuning curve.

1. INTRODUCTION

Doping superlattices with the *n-i-p-i* crystal type structure belong to semiconductor materials with tunable characteristics.¹ They are grown in the process of periodic doping with donor and acceptor impurities of a semiconductor crystal. Main features of the doping semiconductor superlattices are (a) spatial separation of electrons and holes, (b) tunable energy band gap under excitation, and (c) strong changing the energy state structure in dependence on donor and acceptor distribution and concentrations. When the degree of doping or the excitation power of the superlattices change, the structure of their energy levels undergoes reconstruction and, accordingly, widen absorption and luminescence spectra are transformed. At analyzing the transformation of the emission spectra of *n-i-p-i* crystals it is necessary to take into account fluctuations of the concentration of impurities, narrowing of the forbidden band and the impurity correlation effects. Moreover, investigation of the change in the optical and electric characteristics of doping superlattices is of importance in determining the performance efficiency of various optoelectronic devices based on them.

In the present work, the energy and emission spectra of doping superlattices are calculated with allowance for the density-state tails arising as a result of fluctuations of the concentration of impurities. Data of self-consistent calculations of the Schrödinger and Poisson's equations are presented. Transformation of electron energy levels and wave functions and variation of the overlap of electron and hole wave functions under excitation of doping superlattices and in dependence on their design parameters are examined in details. The self-consistent calculations of the characteristic tail parameter and the Coulomb electrostatic potential for the doped layers are performed taking into account correlation in the impurity distribution.^{2,3} Based on the developed method of self-consistent calculations the behavior of tunable optical spectra versus excitation level for doping superlattices of different design is studied. Results of numerical simulation of spectra of emission in the GaSb *n-i-p-i* crystal-based structures are presented and tuning curves for designed laser diodes are examined and discussed.

* Further author information: (Send correspondence to V.K.K.)

V.K.K.: E-mail: lavik@dragon.bas-net.by, Telephone: 375 17 2 840435, Fax: 375 17 2 840879, Web site: <http://www.ac.by/>

D.V.U.: E-mail: UshakovDV@bsu.by, Telephone: 375 17 2 781313, Fax: 375 17 2 121016

I.S.M.: E-mail: manak@bsu.by, Telephone: 375 17 2 781313, Fax: 375 17 2 121016

P.C.: E-mail: christol@cem2.univ-montp2.fr, Telephone: 4 67 523311, Fax: 4 67 544842

A.J.: E-mail: joullie@univ-montp2.fr, Telephone: 4 67 524368, Fax: 4 67 544842

2. STRUCTURE AND MATERIAL PARAMETERS

The basic laser structure is defined for growth on the GaSb substrate.^{4,5} The active region (*n-i-p-i* crystal superlattice) is at the center of the AlGaAsSb waveguide layer of 1 μm -thickness which is surrounded by *n*- and *p*-type cladding layers of 2 μm -thickness. The quaternary alloy material of the waveguide and cladding layer is lattice matched to the substrate. Using size parameters of the doping superlattice layers and corresponding dispersion characteristics, it is possible to evaluate waveguide properties of the active region and to determine the optical confinement factor Γ which determines the loss coefficient and required gain level at lasing.

2.1. Active region with *n-i-p-i* layers

Electronic structure of doping superlattices is determined according to the self-consistent procedure of calculations of the eigen states and wave functions of electrons and holes in quantum wells of the *n-i-p-i* crystal potential relief. Emission spectra depend on populations in the subbands of the quantum wells and the force of optical transitions is rather sensitive to the overlapping of the wave functions. The optical spectra are calculated taking into account the screening of the electrostatic potential and effects of tails of the density of states.¹⁻³

Basic data for calculations of the electronic spectra and emission characteristics of the GaSb *n-i-p-i* crystals include the following parameters. Dopants of *p*- and *n*-type layers are acceptors Be and donors Te, respectively, the crystal constant is $a = 0.61$ nm, energy gap $E_g = 0.727$ eV at temperature $T = 300$ K, dielectric constant $\epsilon = 15.69$, corresponding effective masses of current carriers are equal to $m_c = 0.039m_e$, $m_{vh} = 0.25m_e$, $m_{vl} = 0.044m_e$, $m_{vht} = 0.055m_e$, and $m_{vlt} = 0.115m_e$. The physical parameters related to the sampled GaSb *n-i-p-i* laser structures are given in Tabl. 1. Here, it is presented design parameters (thicknesses of *p*-, *n*-, and *i*-type layers d_p , d_n , and d_i , impurity concentrations N_a and N_d) and electronic state characteristics (the initial potential profile depth $2\Delta V_0$ and effective energy gap of the superlattice E_{g0}') that determine tunability of the emission spectrum of the structure under excitation.

Table 1. Parameters of the GaSb *n-i-p-i* structures and some tunability spectral data.

No.	$d_n = d_p$ (nm)	$N_a = N_d$ (cm^{-3})	$N_d d_n$ (10^{13} cm^{-2})	d_i (nm)	$2\Delta V_0$ (eV)	E_{g0}' (eV)	r	E_g' (eV)	λ' (μm)
1	6.1	10^{18}	0.061	122	0.440	0.287	0.4	0.463	2.678
							0.6	0.551	2.250
							1	0.727	1.705
2	12.2	10^{18}	0.122	61	0.472	0.255	0.4	0.444	2.794
							0.6	0.538	2.304
							1	0.727	1.705
3	12.2	10^{18}	0.122	122	0.901	< 0	0.6	0.367	3.382
							0.8	0.547	2.267
							1	0.727	1.705
4	6.1	3×10^{18}	0.183	61	0.676	0.051	0.6	0.457	2.715
							0.8	0.592	2.095
							1	0.727	1.705

2.2. Potential profile

For determining the potential profile of the *n-i-p-i* crystal, it is preferable to use the approximation of the effective concentrations of impurities.^{1,6,7} In this case, the depth of the superlattice potential profile $2\Delta V$ is determined, for example at $N = N_a d_p - N_d d_n \geq 0$, as

$$2\Delta V = 2\Delta V_0(1-r) = \frac{\pi e^2}{\epsilon} \frac{N_d d_n}{2} (d + d_i)(1-r), \quad (1)$$

where $d = d_n + d_p + 2d_i$ is the superlattice period. Presented data for *n-i-p-i* laser structures Nos. 1–4 demonstrate values of the initial depth of the potential relief $2\Delta V_0$ and effective energy gap E_{g0}' of superlattices and change of the effective energy gap $E_g' = E_g - 2\Delta V$ in dependence on the excitation level of the structures. The excitation factor r is proportional to the non-equilibrium carrier concentration n and is determined as $r = n/N_d d_n$. The amplification of the emission occurs at

the photon energies near the quasi-Fermi level difference ΔF and the related wavelength λ' follows to the effective energy gap E_g' under excitation.^{6,7} As seen, with increasing the excitation r in the range of 0.4 to 0.8 the wavelength of the amplified emission is tuning in the interval 2.7 to 2.1 μm for different structures. Structure No. 3 belongs to a degenerate superlattice and mid-infrared emission at low excitation will be weak.

More detail analysis requires taking into account in calculations appearing nonlinear optical processes in doping semiconductor superlattices at high excitation. Additional ways to control emission characteristics are using the two-section laser structures⁸ or cavity configuration of photonic crystal⁹.

3. STRUCTURE DESIGN AND TUNING CHARACTERISTICS

3.1. Laser structure design

More detail analysis is provided for two possible designed *n-i-p-i* laser structures. Parameters of the active region for design 1 correspond to ordinary configuration of *n*- and *p*-type layers, i. e., $N_a = 10^{19} \text{ cm}^{-3}$, $N_d = 10^{18} \text{ cm}^{-3}$, $d_p = 8.54 \text{ nm}$, $d_n = 20.13 \text{ nm}$, $d_i = 1.22 \text{ nm}$, $d = 31.11 \text{ nm}$. The active region for design 2 includes δ -doped *n*- and *p*-type layers, i. e., the parameters are $N_a = N_d = 5 \times 10^{19} \text{ cm}^{-3}$, $d_p = d_n = 1.83 \text{ nm}$, $d_i = 8.54 \text{ nm}$, $d = 20.74 \text{ nm}$. The potential relief of the superlattices of these different designs is shown in Fig. 1. Selection of the impurity concentrations and mode of their introducing into the layers determines the behavior of the potential relief under the structure excitation and respectively the change in the energy set of emitted quanta $h\nu$ and variation in the probability of different optical transitions.

The probability of optical transitions is mainly determined by the overlapping of the wave functions of electrons and holes occupying states in the potential relief quantum wells.¹ A set of the squared overlap integrals for most effective transitions for the structures with designs 1 and 2 is presented in Fig. 2. The calculations have been done in the self-consistent manner and include transitions between various states in the subbands and minibands of spatially separated electron and hole quantum wells. According obtained results, we can conclude that the δ -doped superlattices are most suitable for the realization of high enough optical oscillator forces and for the receiving a medium with a widen tunable electronic structure in the active region.

3.2. Emission spectra and recombination rate

The radiative recombination rate R_{lum} is determined by integration of the spectral radiative recombination rate $r_{\text{lum}}(h\nu)$ all over the photon energies $h\nu$ at definite difference between the quasi-Fermi levels ΔF and the crystal temperature T . The values of $r_{\text{lum}}(h\nu)$ are connected with spectral spontaneous recombination rate $r_{\text{sp}}(h\nu)$ by the expression

$$r_{\text{lum}}(h\nu) = \frac{1 - \exp(-\Delta F / kT)}{1 - \exp(-h\nu / kT)} r_{\text{sp}}(h\nu). \quad (2)$$

The expression for $r_{\text{sp}}(h\nu)$ in the \mathbf{k} -selection rule model has the form¹

$$r_{\text{sp}}(h\nu) = \frac{A_{\text{cv}}}{\pi \hbar^2 N_p d} \sum_i m_{\text{rit}} \sum_n \sum_m \sum_v H_t(h\nu - h\nu_{nmiv}) I_{nmiv}^2 f_e(E_{cnmiv}) f_h(E_{vnmiv}). \quad (3)$$

Here, A_{cv} is the Einstein coefficient, N_p is the number of the superlattice periods, I_{nmiv} is the overlap integral of the envelop wave functions of electrons and holes, $f_e(E_{cnmiv})$ and $f_h(E_{vnmiv})$ are the Fermi–Dirac functions for electrons and holes,

$$E_{cnmiv} = E_{c0} + \frac{m_{\text{rit}}}{m_c} (h\nu - E_g') + \frac{m_{\text{rit}}}{m_{\text{vit}}} E_{cnv} - \frac{m_{\text{rit}}}{m_c} E_{vimv}, \quad (4)$$

$$E_{vnmiv} = E_{v0} - \frac{m_{\text{rit}}}{m_{\text{vit}}} (h\nu - E_g') + \frac{m_{\text{rit}}}{m_{\text{vit}}} E_{cnv} - \frac{m_{\text{rit}}}{m_c} E_{vimv}, \quad (5)$$

m_c is the effective mass of electrons, m_{vit} is the effective mass transverse component for heavy ($i = h$) and light ($i = l$) holes, $m_{rit} = m_c m_{vit} / (m_c + m_{vit})$ is the reduced mass, E_{c0} and E_{v0} are the energies of the bottom of the conduction band and top of the valence band. The summation in Eq. (3) is performed over the quantum numbers of minibands v , electron n and hole subbands m . Transitions between the subbands of electrons and holes begin at the light quanta $h\nu_{nmiv} = E_g^i + E_{cnv} + E_{vimv}$ which is concerned with the effective band gap of the doping superlattice $E_g^i = E_{c0} - E_{v0}$ and the ground states of the subbands E_{cnv} and E_{vimv} .

The function $H_t(y)$ is determined by the energy spectra broadening. If the broadening effects in a semiconductor structure are negligible, $H_t(y)$ is represented by the Heaviside unit-step function. For heavily doped superlattices, the impurity and intrinsic bands are to be overlapping. Therefore, tails of the density of states appear.^{1,2} In the case of the Gaussian-like tails the function $H_t(y)$ has the form $H_t(y) = \text{erfc}(-y/\sigma_{cv})/2$.³ Here, $\sigma_{cv} = \sqrt{\sigma_c^2 + \sigma_v^2}$, σ_c and σ_v are the characteristic tail parameters of the density of electron and hole states which decrease with the increase of excitation level of the superlattice.¹⁻³

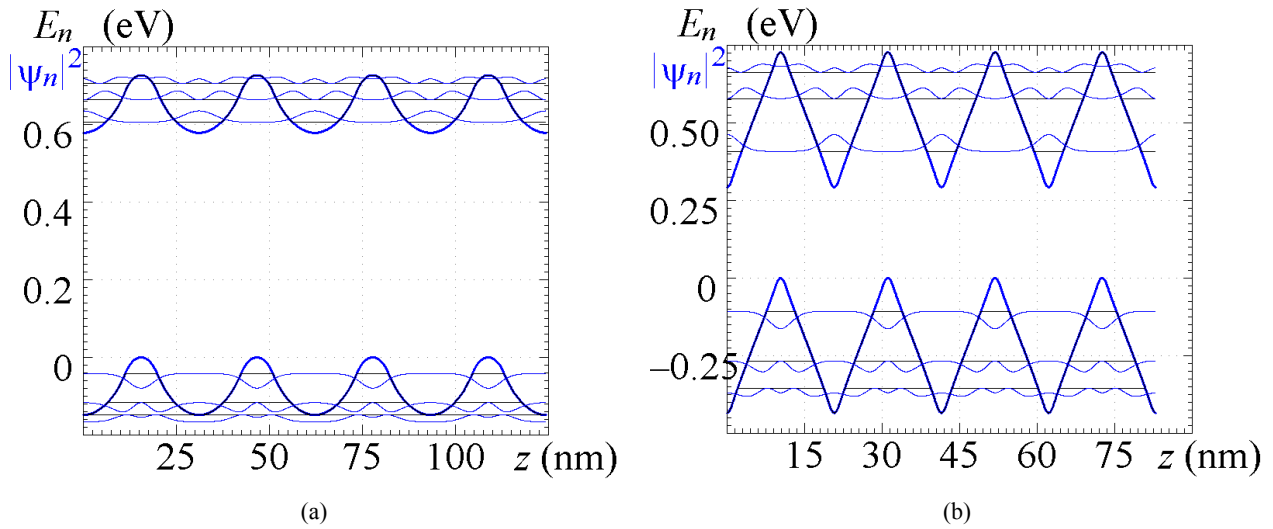


Figure 1. Band diagram of the structures along the z -axis of quantization, energy levels E_n and squared wave functions $|\psi_n|^2$ for structure designs (a) 1 and (b) 2. $\Delta F = 0.6$ eV.

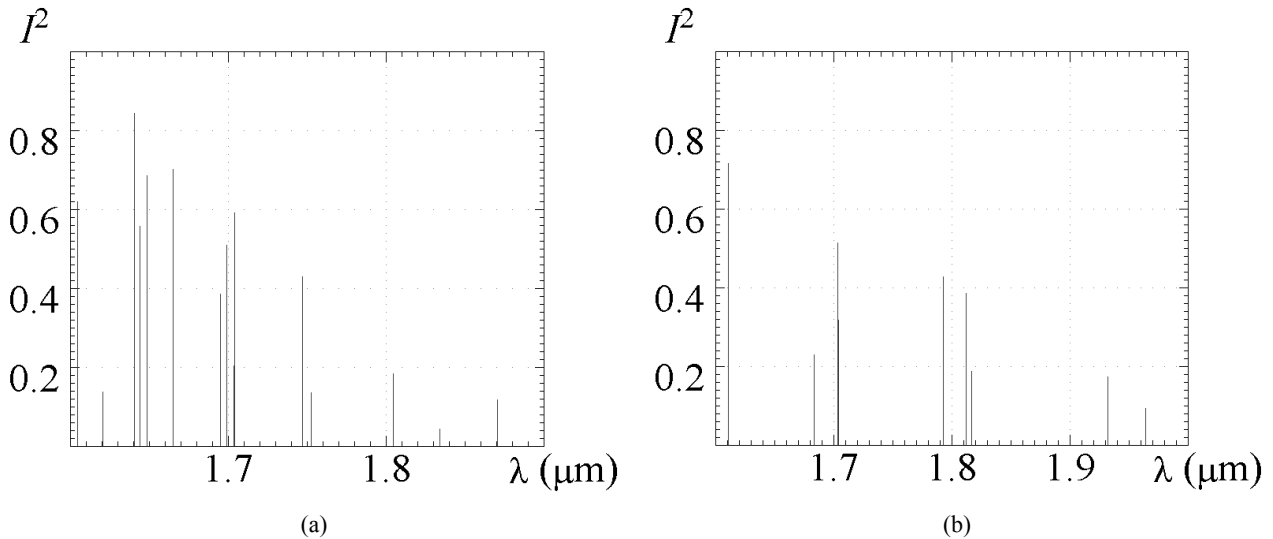


Figure 2. Squared overlap integral I^2 of the wave functions at various optical transitions corresponding to the wavelength λ for structure designs (a) 1 and (b) 2. $\Delta F = 0.7$ eV.

The gain coefficient $k_g(\nu)$ is connected with the spontaneous emission rate $r_{sp}(h\nu)$ by means of the universal relation¹

$$k_g(\nu) = \frac{1}{\nu\rho} \left(1 - \exp\left(\frac{h\nu - \Delta F}{kT}\right) \right) r_{sp}(h\nu). \quad (6)$$

Here $\rho(h\nu) = 8\pi(h\nu n_r)^2/c^2 h^3 \nu$ is the density of electromagnetic modes, n_r is the refractive index, ν is the light velocity in the semiconductor crystal. Therewith, the radiation is considered to be isotropic.

3.3. Gain spectra and tuning curves

Gain spectra of the designed laser structures are calculated according probated software.¹ The method of the calculations takes into account of appeared tails of the density of states, screening effects, and self-consistent transformation of the electronic states and wave functions under excitation of the superlattice. Change in the gain spectrum $k_g(\nu)$ is shown in Fig. 3.

The presented values of the gain k_g are not including the optical confinement factor Γ . The value of the confinement factor depends on the number of superlattice periods and dispersion characteristics of the active, waveguide, and cladding layers of the laser diode. Calculated values of the confinement factor Γ for different laser structure designs (1 and 2) and in dependence on the number of the superlattice periods N_p are given in Tabl 2. An example of the intensity distribution of the electromagnetic wave in the active region is presented in Fig. 4.

Table 2. Values of the optical confinement factor Γ for the GaSb *n-i-p-i* laser structures.

N_p		2	4	6	8	10	12
Γ	Design 1	0.1153	0.3476	0.5555	0.7017	0.7975	0.8601
	Design 2	0.0542	0.1879	0.3466	0.4918	0.6097	0.7003

Tuning curves are calculated for laser diodes which wavelength of the emission is selected in the external cavity, such as the Littman and Metcalf configuration.¹⁰ Trace gas detection with similar tunable sources is easily provided with a multipass cell.¹¹ The calculation procedure of the tuning curves includes the determination of the sheet photon density S in the active region of the laser source. It is defined as

$$S = \frac{1}{\nu k_1} \left(\frac{j}{e} - \left(R_{lum} d + \frac{n}{\tau_{nr}} \right) N_p \right), \quad (7)$$

where j is the current density, k_1 is the loss coefficient. The value τ_{nr} is introduced for describing a contribution of the nonradiative recombination process and it can be considered to be of 1 μs .⁶⁻⁸ In a selective cavity, the lasing wavelength λ corresponds to the equation

$$\Gamma k_g(\lambda) = k_1. \quad (8)$$

For simplicity, selection of the lasing wavelength is examined in the conditions where Γ and k_1 do not markedly change within the gain spectrum and the pump current density j of the tunable laser source is fixed.

Results of the calculated tuning curves are presented in Fig. 5. As seen, it is possible for designed laser structures to obtain the lasing wavelength tuning from 1.6 to 2.2 μm with the control of the excitation level. The tuning curve depends on the number of periods of the superlattice in the active region and more wide range of the tuning at room temperature is expected for *n-i-p-i* structures with high-doped δ -layers. For structure 1, with increasing the number of superlattice periods N_p maximum of the photon density decreases. For structure 2, optimal tuning curve is observed at $N_p = 8$.

4. CONCLUSION

Using of the developed method of self-consistent calculations provides the detailed description of tunable optical spectra versus excitation level for the GaSb doping superlattices of different design. Results of numerical simulations give

spectra of the emission in the GaSb *n-i-p-i* crystal structures and corresponding tuning curves for designed laser diodes. For the GaSb-based lasers with *n-i-p-i* layers in the active region, it is possible to obtain the emission wavelength tuning from 1.6 to 2.2 μm in a selective cavity with increasing the pump current. The tuning curve depends on the number of periods of the superlattice and more wide range of the tuning at room temperature is expected for *n-i-p-i* structures with high-doped δ -layers.

ACKNOWLEDGMENTS

The work was supported under collaboration project by CNRS (France) and NASB (Belarus). The authors are also thankful to A. A. Afonenko for useful discussions and remarks.

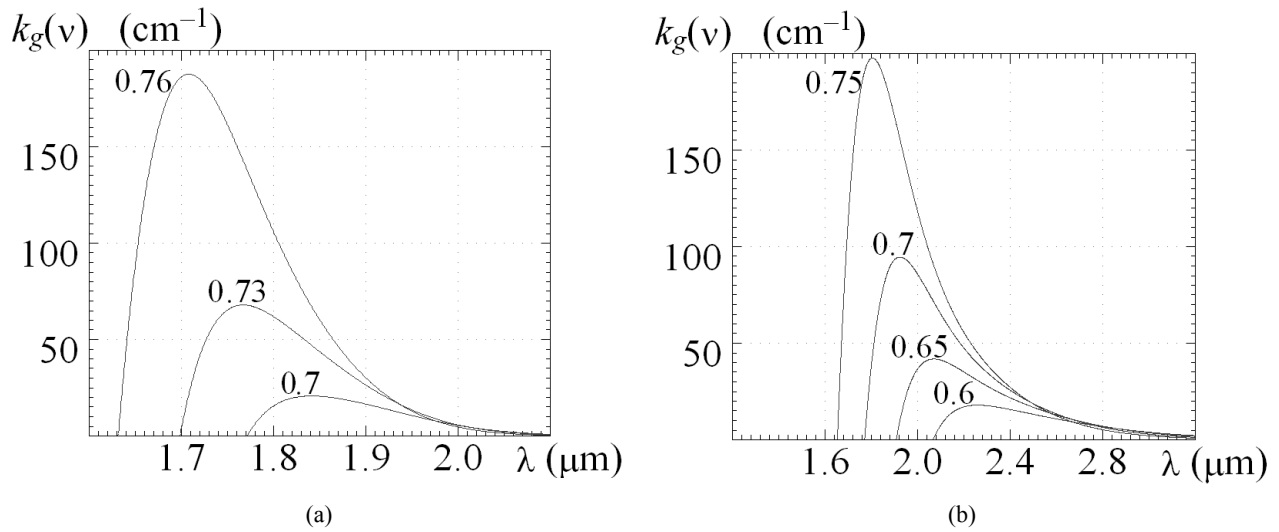


Figure 3. Gain spectra $k_g(\nu)$ of *n-i-p-i* structures with design (a) 1 and (b) 2 at different ΔF (figures at the curves in eV).

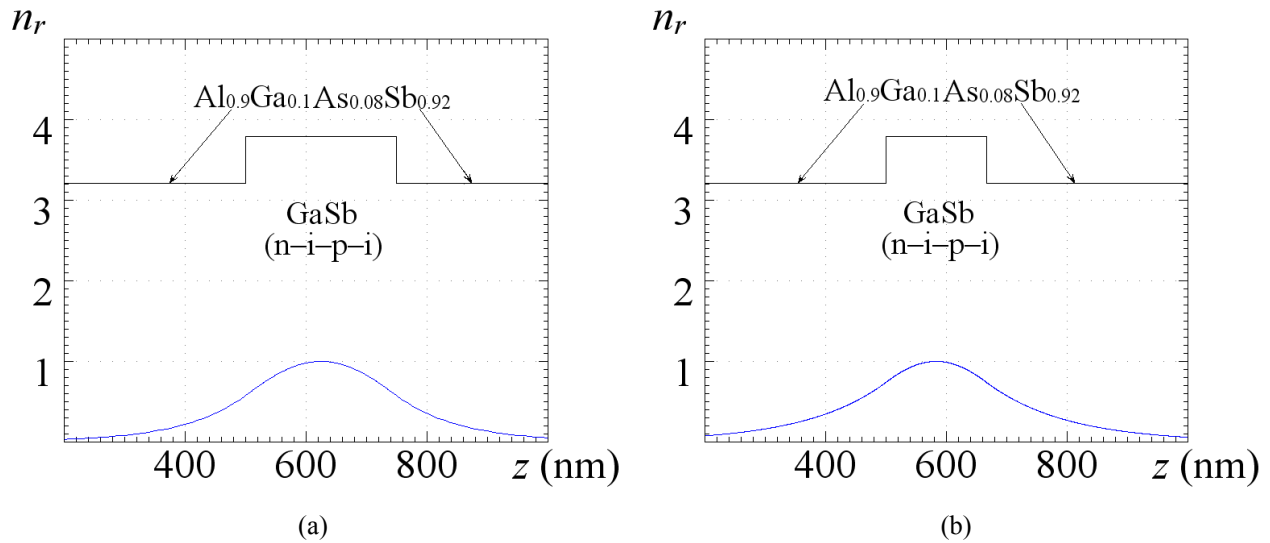


Figure 4. Refractive index n_r and light intensity distribution for structure designs (a) 1 and (b) 2. $N_p = 8$.

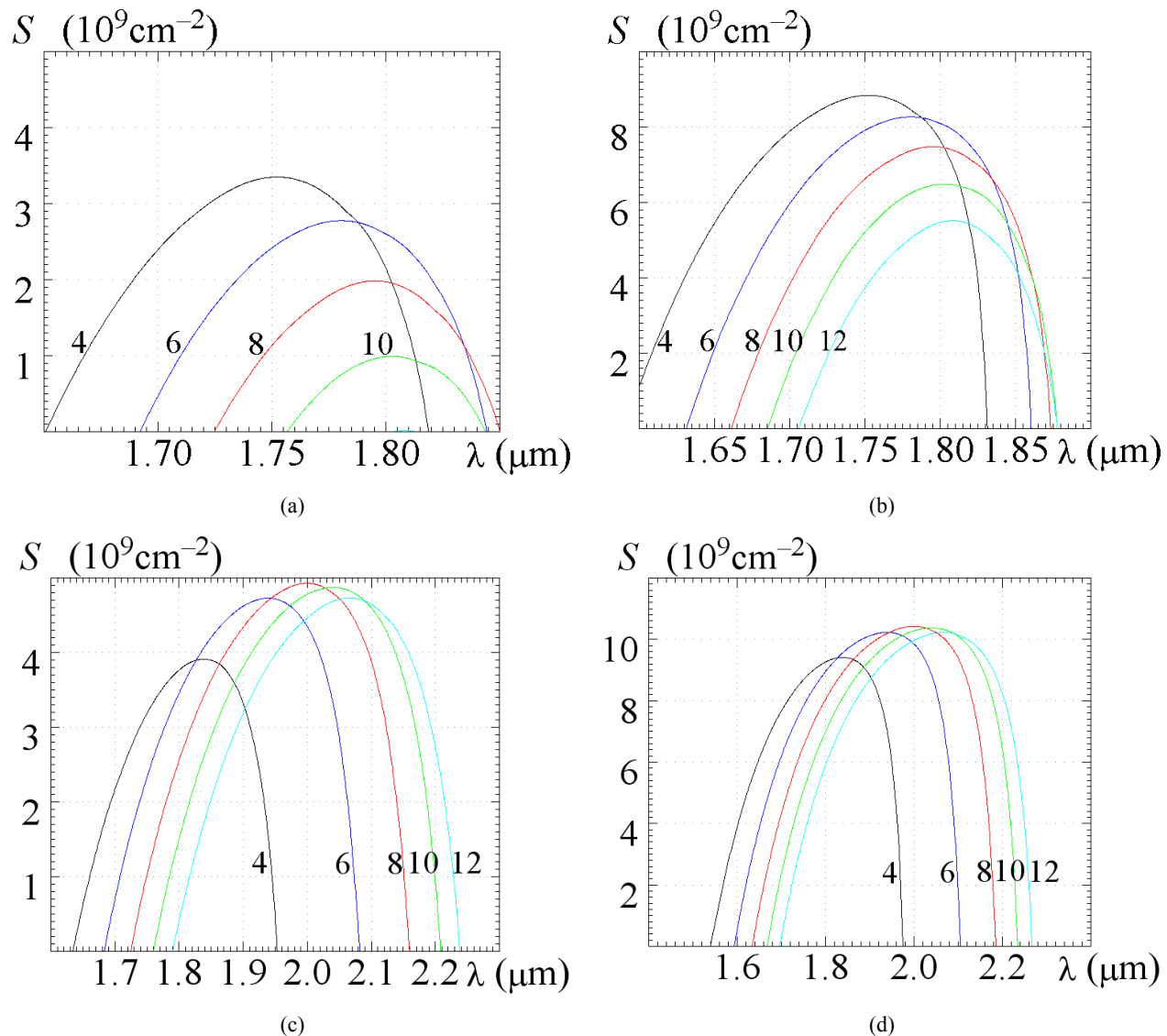


Figure 5. Tuning curves $S(\lambda)$ versus numbers of the superlattice period (figures at the curves) for laser structures with different designs (a, b) 1 and (c, d) 2. $k_1 = 30 \text{ cm}^{-1}$, (a, c) $j = 300 \text{ A/cm}^2$ and (b, d) $j = 500 \text{ A/cm}^2$.

REFERENCES

1. V. K. Kononenko, I. S. Manak, and D. V. Ushakov, "Optoelectronic properties and characteristics of doping superlattices," *Proc. SPIE* **3580**, pp. 10-27, 1998.
2. V. K. Kononenko and D. V. Ushakov, "Carrier transport and screening in $n-i-p-i$ crystals," *Phys. stat. sol. (b)* **211**, pp. 743-749, 1999.
3. D. V. Ushakov, V. K. Kononenko, and I. S. Manak, "Effects of energy-spectrum broadening in alloyed semiconductor superlattices," *J. Appl. Spectrosc.* **66**, pp. 820-825, 1999.
4. A. Joullié and P. Christol, "GaSb-based mid-infrared 2–5 μm laser diodes," *C. R. Physique* **4**, pp. 621–637, 2003.
5. A. Joullié, P. Christol, A. N. Baranov, and A. Vicet, "Mid-infrared 2–5 μm heterojunction laser diodes," *Topic Appl. Phys.* **80**, pp. 1–59, 2003.
6. V. K. Kononenko, H. W. Kunert, I. S. Manak, and D. V. Ushakov, "Tunable photoluminescence spectra of doped semiconductor superlattices," *J. Appl. Spectrosc.* **70**, pp. 115-121, 2003.

7. V. K. Kononenko, D. V. Ushakov, and H. W. Kunert, "Effects of doping and nonradiative defects in GaAs superlattices," in *Physics, Chemistry and Application of Nanostructures*, pp. 55-58, World Scientific, Singapore, 2003.
8. D. V. Ushakov, V. K. Kononenko, and I. S. Manak, "Radiative characteristics of a two-section laser structure based on a δ -doping superlattice," *Opt. & Spectrosc.* **94**, pp. 469-475, 2003.
9. A. G. Smirnov, D. V. Ushakov, and V. K. Kononenko, "Multiple-wavelength lasing in one-dimensional band gap structures: implementation with active *n-i-p-i* layers," *J. Opt. Soc. Am. B* **19**, pp. 2208-2214, 2002.
10. V. K. Kononenko, I. S. Manak, and S. V. Nalivko, "Design and characteristics of widely tunable quantum-well laser diodes," *Spectrochimica Acta, Part A: Mol. & Biomol. Spectrosc.* **55**, pp. 2091-2096, 1999.
11. A. Vicet, D. A. Yarekha, A. Pérona, Y. Rouillard, S. Gaillard, and A. N. Baranov, "Trace gas detection with antimonide-based quantum-well diode lasers," *Spectrochimica Acta Part A: Mol. & Biomol. Spectrosc.* **58**, pp. 2405-2412, 2002.